Journal of The Electrochemical Society, **149** (10) A1293-A1298 (2002)
0013-4651/2002/149(10)/A1293/6/$7.00 © The Electrochemical Society, Inc.

In Situ Potential-Dependent FTIR Emission Spectroscopy

A Novel Probe for High Temperature Fuel Cell Interfaces

Xinyu Lu,* Peter W. Faguy, and Meilin Liu**,z**

Center for Innovative Fuel Cell and Battery Technologies, School of Materials Science and Engineering, Georgia Institute of Technology, Atlanta, Georgia 30332, USA

Potential-dependent Fourier transform infrared emission spectroscopy (pd-FTIRES) has been used for the first time to study, *in situ*, oxygen reduction under practical operating conditions of intermediate-temperature solid oxide fuel cells. Surface emission difference spectra of functioning cathodes at 550°C under a variety of feed gas conditions and overpotentials were obtained. Various surface oxygen anions were observed on the cathode surface under specific oxygen concentrations. The interfacial structural data were also correlated to ac impedance and chronoamperometric measurements. In addition to the bands associated with adsorbed oxygen anions, broad spectral features arising from the electrochemical polarization were also observed. These spectral features are believed to be due to electrochemically induced changes in the optical properties of the emitting surface layer.
 [DOI: 10.1149/1.1503961]

Manuscript submitted April 19, 2002; revised manuscript received June 17, 2002. Available electronically August 15, 2002.

It is well known that the key issues facing solid oxide fuel cell (SOFC) technology are cost reduction and minimization of internal electrochemical losses. As the operating temperature is reduced, many cell components such as the interconnect and heat exchangers can be fabricated from much less expensive materials, technical difficulties will find easy solutions, and system reliability, operational life, and the possibility of using SOFCs for a wide variety of applications increase. Unfortunately, the interfacial polarization resistances increase dramatically as the operating temperature is reduced; this is especially true for oxygen reduction at the cathode. In fact, the performance of a low-temperature SOFC is most severely limited by the polarization resistances at the cathode/electrolyte interface.[1,2]

While considerable efforts have been devoted to the development of efficient cathode materials, a detailed understanding of the chemistry and electrochemistry at SOFC cathode surfaces is still lacking. The significance of each elementary step involved in oxygen reduction in SOFCs, such as adsorption, dissociation, charge transfer, and mass transfer, is still not clear. Thus, it is imperative to elucidate the reaction mechanism of oxygen reduction in order to more effectively optimize cathode performance.

A spectroscopic technique that can provide structural details under conditions of actual fuel cell operation is extremely attractive. Fourier transform infrared spectroscopy (FTIR) has been widely used for *in situ* analysis of adsorbed species and surface reactions. A significant body of work exists on utilizing emission spectroscopy to characterize oxide surfaces.[3-5] There also exists a twenty year history of applying infrared spectroscopy to the study of electrochemical interfaces.[6] Our work is a natural extension of those two traditions. A new tool has been developed in our laboratories, and applied to the study of oxygen reduction at SOFC cathodes. This newly developed hybrid technique, potential dependent FTIR emission spectroscopy (pd-FTIRES), provides structural information as to the extent and nature of oxygen species adsorbed on the cathode surface and also for the electrode material itself, all as a function of temperature, overpotential, and oxygen partial pressure.

The purpose of this communication is to introduce pd-FTIRES and to rationalize the pd-FTIRES spectra correlated to electrochemical data with the types of the intermediate species involved in oxygen reduction found at the interfaces. This new technique will have a great impact on future studies of gas/solid interactions in solid-state electrochemical systems.

* Electrochemical Society Student Member.
** Electrochemical Society Active Member.
z E-mail: meilin.liu@mse.gatech.edu

Experimental

Materials and electrode preparation.—An intermediate-temperature cathode material, $Sm_{0.5}Sr_{0.5}CoO_{3-\delta}$ (SSC), and an electrolyte material $Sm_{0.2}Ce_{0.8}O_{2-\delta}$ (SDC) were prepared by the glycine-nitrate process.[7] The resulting SDC powder was pressed into pellets under 400 atm for 1 min and sintered in air at 1400 ~1500°C for 5 h to achieve sintered densities greater than 95% of the theoretical values. The as-sintered SDC pellets (with 8 mm in diam and 0.4 mm thickness) were ground and polished to ensure surface smoothness. The SSC powder and a binder (V-006, Heraeus) were screen printed on both sides of the as-polished SDC pellets and fired at 1000°C for 4 h to form porous SSC layers (~10 μm). The microstructures of the samples were examined using a scanning electron microscope (SEM, Hitachi S-800) and the micrographs of the cathode for an SSC|SDC|SSC trilayer are shown in Fig. 1. Au ink was painted to the edges of both SSC electrodes and fired at 800°C for 30 min as the current collector.

Spectroelectrochemical cell.—The sample is placed on the top of a stainless steel sample cup mounted to a metal fixture that contains a heating cartridge. The top surface center of the sample is positioned accurately at the short ellipsoid focus. An aperture and the tiltable sample holder are used to adjust the intensity of the emission from the sample. KBr is used for all windows in the optical path. N_2 (ultrahigh purity, $[O_2] \sim 10$ ppm, estimated from a zirconia oxygen sensor measurement), 1% O_2 balanced in N_2, and air (breathing grade) are all from Air Products, Inc. Mass flow controllers are used to maintain the constant gas flows (~50 mL min^{-1}) to both sides of the sample. A thermocouple is positioned on the top rim of the sample cell to monitor the temperature. The sample temperature is automatically controlled to within 1°C.

Figure 2 shows a schematic diagram of the optical configuration used for the emission measurements. The spectroelectrochemical cell was placed on the top of the sample cup in a Praying Mantis diffuse reflectance sampling accessory equipped with a high temperature reaction chamber. The Praying Mantis attachment was positioned at an emission port on the Bruker Equinox 55 FTIR spectrometer. The top surface of the electrode (0.13 cm^2) then becomes the source of infrared light modulated by the interferometer. While the transfer optics are not perfectly optimized, the electrode surface is at the focal point of the ellipsoidal optics in the diffuse reflectance attachment and the *f* number for the focusing mirror in the emission port is small, therefore light levels reaching the detector are high enough for high quality spectra.[8]

Electrochemical measurements.—An EG&G 273A potentiostat/galvanostat and a 5201 lock-in amplifier were used to collect ac impedance spectra and apply dc potentials to the cell. The frequency

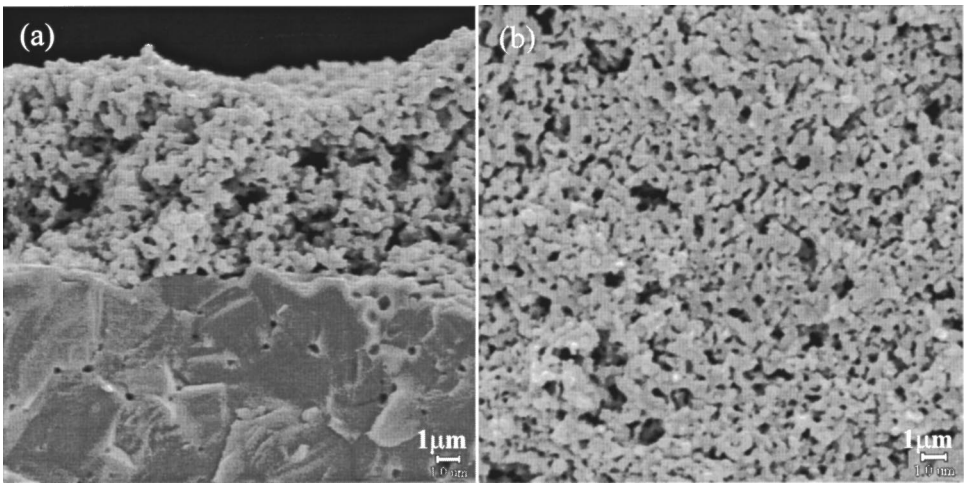

Figure 1. Scanning electron micrographs of the cathode side of a symmetrical cell, SSC|SDC|SSC, used in the pd-FTIRES measurements: (a) cross-sectional and (b) top-down view of the SSC surface.

range of impedance measurements was from 0.01 Hz to 100 kHz, and the amplitude of the input sine wave signal was 5 mV. Ag wires were connected to the two electrodes through the Au current collectors and led to the potentiostat/galvanostat. The bulk resistances of the cell were measured using impedance spectroscopy at each point in order to correct the ohmic loss across the electrolyte in dc polarization measurements. All dc measurements were acquired in a steady state; it took about 3-10 min for the system to reach equilibrium under each testing condition. The salient electrochemical parameters are listed in Table I.

Spectroscopic measurements.—A liquid nitrogen cooled mercury-cadmium-telluride detector was used with a Ge-coated KBr beam splitter and a mirror speed of 20 kHz. Single beam emissivity curves were collected at 4 cm^{-1} resolution coadding 128 scans into each interferogram. Spectra were collected at open circuit voltage (OCV), then the potential was fixed across the cell, after the transient current decayed spectral collection proceeded. This cycle was repeated for each sample potential, typically 100-200 mV increments over a 1.5 V range of applied potentials. This corresponded to 30-160 mV increments over 0.8 V for the overpotentials, after the correction of ohmic drop across the electrolyte was applied.

Spectroscopic data are presented as emittance difference spectra, as given in Eq. 1

$$\Delta\varepsilon/\varepsilon_o(\%) = \frac{\varepsilon(\bar{\nu},T,V_i)}{\varepsilon_o(\bar{\nu},T,V_o)} - 1 \qquad [1]$$

where the single beam emittance spectrum, $\varepsilon(\bar{\nu})$, is a function of temperature and applied potential. Calculating the pd-FTIRES spectra provides both a method to clearly identify the spectral features associated with the electrochemically induced structural changes and to reject the instrument lineshape function which is dominated by the emissivity profile of this pseudo-blackbody emitter. This is an important point; the difference spectra are affected indirectly, not directly, by the operating temperature of the sample or source. The indirect effects stem from the effect of temperature on ion transport and electrode kinetics, direct effects due to the emissivity of the sample are canceled by using the spectra obtained under open-circuit conditions, $\varepsilon_0(\bar{\nu})$, as essentially a blackbody reference. For convenience, the pd-FTIRES spectra are presented in dimensionless percent units.

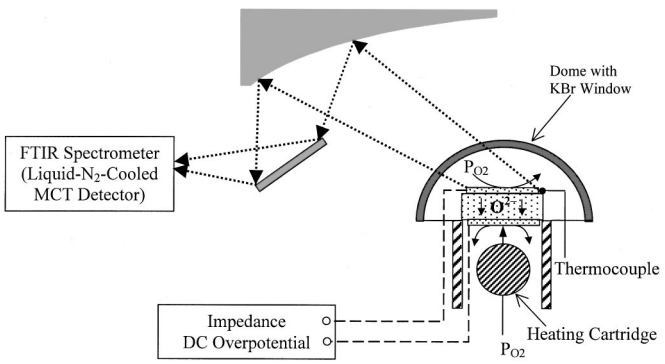

Figure 2. Schematic diagram of optical configuration for pd-FTIRES experiments.

Table I. Electrochemical parameters for pd-FTIRES measurements of a symmetrical cell, SSC|SDC|SSC, at 550°C for various feed gases. R_b represents the bulk resistance of the electrolyte (SDC), whereas R_p represents the interfacial polarization resistance between SSC and SDC under open circuit voltage (OCV).

	Applied voltage (V)	Overpotential (mV)	Current density (mA cm^{-2})
In air	0.0	0	0.0
R_b = 0.40 Ω cm^2	−0.10	−38.0	−76.98
R_p = 0.24 Ω cm^2			
at OCV	−0.30	−109	−237.3
	−0.50	−174	−404.0
	−0.70	−232	−580.2
	−0.90	−277	−772.2
	−1.2	−317	−1095
	−1.5	−323	−1460
In 1% O_2	0.0	0	0.0
R_b = 0.40 Ω cm^2	−0.10	−61.0	−49.21
R_p = 0.65 Ω cm^2			
at OCV	−0.30	−178	−150.8
	−0.50	−295	−254.8
	−0.70	−420	−346.8
	−0.90	−584	−391.3
	−1.0	−672	−406.3
	−1.1	−758	−424.6
In N_2			
($[O_2] \sim 10$ ppm)	0.0	0	0.0
R_b = 0.40 Ω cm^2	−0.20	−199	−1.040
$R_p \rightarrow \infty$ at OCV	−0.30	−299	−1.254
	−0.40	−399	−1.460
	−0.50	−498	−2.286
	−0.60	−597	−4.079
	−0.70	−693	−8.143

Results and Discussion

An important consideration in interpreting pd-FTIRES, or any difference emittance spectra, is that any positive-going feature represents an increase in emittance at that frequency for the sample relative to the reference and vice versa. These excursions are caused by a change in concentration of an emitting species at the surface of the emission sample, due to either faradaic processes consuming or producing the emitter or by potential-induced adsorption/desorption phenomena. These spectra features are analogous to the bands seen in subtractively normalized interfacial FTIR and pd-FTIR reflection absorption spectroscopy experiments.[5]

An additional phenomenon also appears to be occurring where the emission characteristics of the electrode surface layer vary with applied potentials. This is analogous to the electroreflectance phenomena found in electrochemically modulated UV-visible reflectance measurements, where the optical constants of the electrode itself are modulated by the applied electric field.[9] This electroemission phenomenon has not previously been observed.

As the pd-FTIRES spectra shown in Fig. 3 indicate, both of these types of spectral features, as described above can be found. The negative-going features around 1250-900 cm^{-1} can be ascribed to the disappearance of surface superoxide moieties as the electrode overpotential is made more cathodic. The broad baseline shifts that are highly dependent on feed gas compositions also show a potential dependency. These broad features are not temperature induced, as all data was taken at 550°C. The shapes of the pd-FTIRES spectra are consistent with frequency dependent changes in the emissivity of the surface, induced by the change in applied potential.

Although free molecular oxygen in a gas phase is not infrared active (since it is centrosymmetric or nonpolar), oxygen molecules or ions adsorbed on the surface of an electrode (metallic or mixed-conducting), under the influence of an applied electrical field, are polarized and become infrared active. The oxygen reduction at the cathode of an SOFC involves a series of elementary steps, including gas-phase diffusion of O_2 to the cathode surface, adsorption and dissociation of oxygen molecules, surface diffusion, charge transfer, and ionic diffusion through a mixed conducting electrode and into the electrolyte. Some equilibria are likely involved among the various surface oxygen species

$$O_{2(gas)} \leftrightarrow O_{2(adsorbed)} \leftrightarrow O_2^- \leftrightarrow O_2^{2-} \leftrightarrow O^- \leftrightarrow O^{2-} \qquad [2]$$

FTIR can render valuable information concerning the forms of adsorbed oxygen, such as peroxide ions O_2^{2-} (800-900 cm^{-1}), superoxide ions O_2^- (1040-1190 cm^{-1}), and adsorbed O_2 (1500-1700 cm^{-1}).[10-14]

Shown in Fig. 4 are the pd-FTIRES spectra recorded for a symmetric cell, SSC/SDC/SSC, in air, 1% oxygen, and in N_2 for various applied potentials. The local baselines have been corrected with cubic polynomial fits between 1435 and 830 cm^{-1}. This was done to separate out the electroemission effect from the adsorbate mode changes. As a comparison of the three stack plots indicates, changes in partial pressure of oxygen, and the cathodic overpotential induced remarkable spectral changes.

The pd-FTIRES spectra obtained at 550°C under cathodically polarized conditions showed a very strong absorption band at about 1124 cm^{-1} and two weak absorption bands at 1236 and 930 cm^{-1} (near the high frequency tail and low frequently tail of the 1124 cm^{-1} band), respectively. The strong band at 1124 cm^{-1} and the weak band around 1236 cm^{-1} are assigned to normal and perturbed superoxide ions (O_2^-), respectively.[10] The weak band around 930 cm^{-1} is assigned to peroxide ions (O_2^{2-}), again based on analogous assignments in the literature.

Figure 5 shows the normalized peak heights as a function of overpotential for these three bands for the oxygen limited feed gas experiments. All three modes in both feed gases show identical potential dependencies. This is puzzling, as all three modes have been assigned to different adsorbate species; this means that the coverage of three distinct molecular species all follow the same potential dependency. It could be that three distinct surface-bound dioxygen species, intermediate in charge density between molecular oxygen and peroxide, exist. It is inviting to assign them to oxygen vacancy, divalent, and trivalent cation sites, but again, their identical potential dependence is puzzling.

As another indication of the power of *in situ* structural data, it is

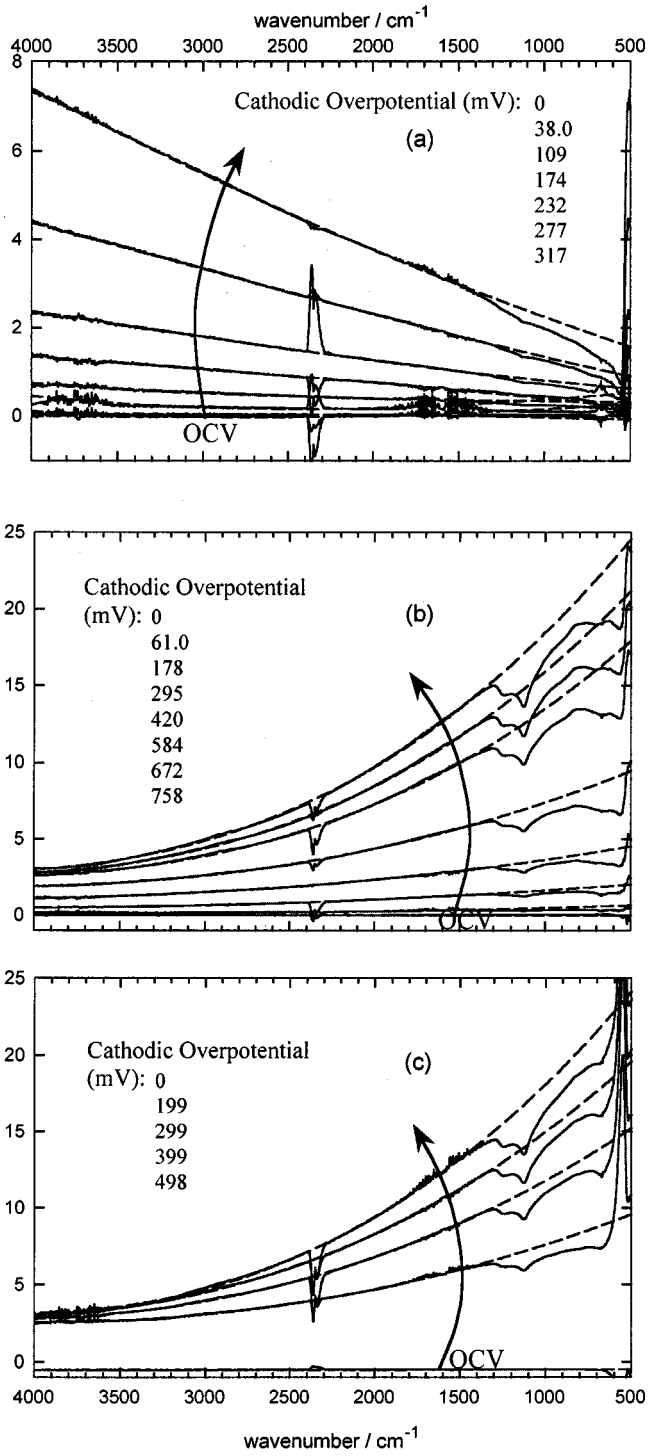

Figure 3. Comparison of pd-FTIRES spectra for three different feed gas conditions: (a) air, (b) 1% O_2 in N_2, and (c) N_2. Dashed lines indicate cubic polynomial fits to baselines. Electrochemical characteristics are listed in Table I. The arrows indicate the increasing direction of cathodic overpotentials.

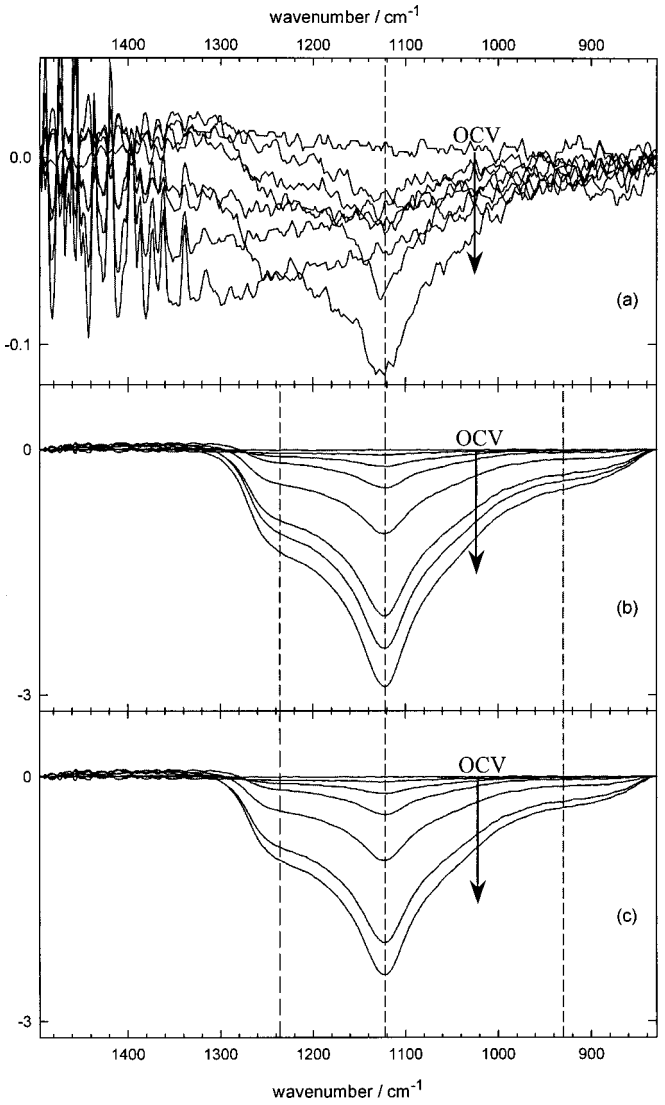

Figure 4. Comparison of pd-FTIRES spectra after local baseline correction for three different feed gas conditions: (a) air, (b) 1% O_2 in N_2, and (c) N_2. Overpotential excursions range from (a) 0 to 320 mV, (b) 0 to 760 mV, and (c) 0 to 690 mV. The arrows indicate the increasing direction of cathodic overpotentials.

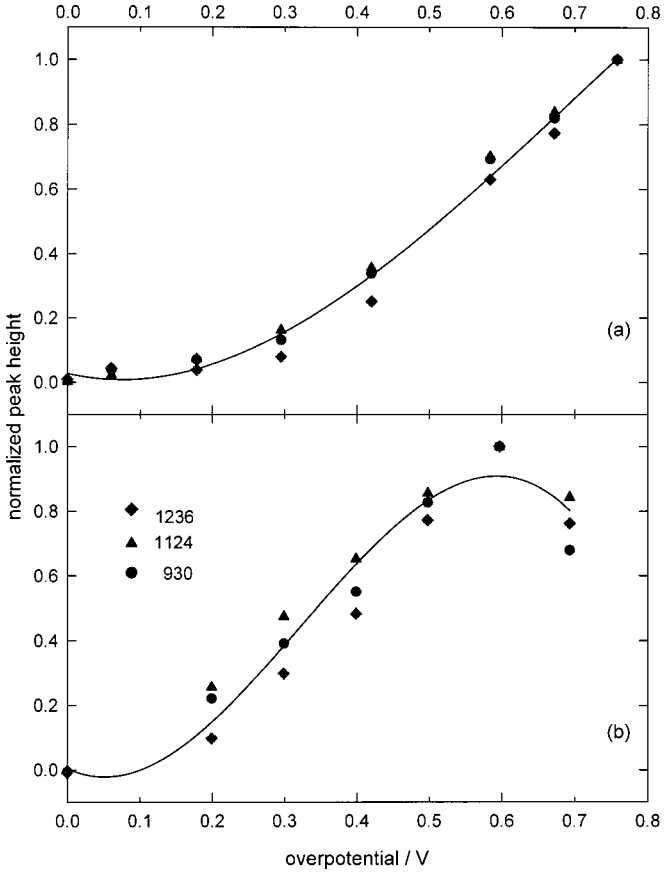

Figure 5. Normalized peak heights (relative to maximum peak heights in series) for superoxide modes (see Fig. 4) as a function of cathode overpotential for two different feed gas conditions: (a) 1% O_2 in N_2 and (b) N_2.

possible to further analyze the peak height data. If the peak heights relative to the largest peak in the spectra, the 1124 cm^{-1} band, are plotted as function of overpotential an informative trend is found. Figure 6 shows the relative peak heights as a function of overpotential for the two oxygen deficient environments. For both the 1236 and 930 cm^{-1} modes and for both gas feed conditions, the relative peaks approach a constant value as the electrode is polarized cathodically. However, while both the higher frequency bands and the low frequency band for the 1% O_2 case all approach a relative peak height of ~0.42, the 930 cm^{-1} band for the N_2 environment approaches approximately half that value. This is a clear indication that the species responsible for the 930 cm^{-1} emission is not the same as those (or that one) responsible for the other bands, and varies in initial OCV coverage with respect to the superoxide species as a function of gas environment.

Qualitatively then, on the cathode surface, superoxide ions (O_2^-) adsorb at or near positively charged reactive sites, such as $V_O^{\cdot\cdot}$, Co^{2+}, and Sm^{3+}, forming bonds as $V_O^{\cdot\cdot}$—O_2^-, Co^{2+}—O_2^- and Sm^{3+}—O_2^- in a dynamic-equilibrium state. When a cathodic overpotential is applied, electrons are injected to these reactive sites and transferred to the O_2^-, inducing a series of reactions to occur, possibly following $O_2^- \leftrightarrow O_2^{2-} \leftrightarrow O^- \leftrightarrow O^{2-}$. As shown in Fig. 4, the negative-going features around 1250 to 900 cm^{-1} grow largely (more negative) with increasing cathodic overpotentials, indicating

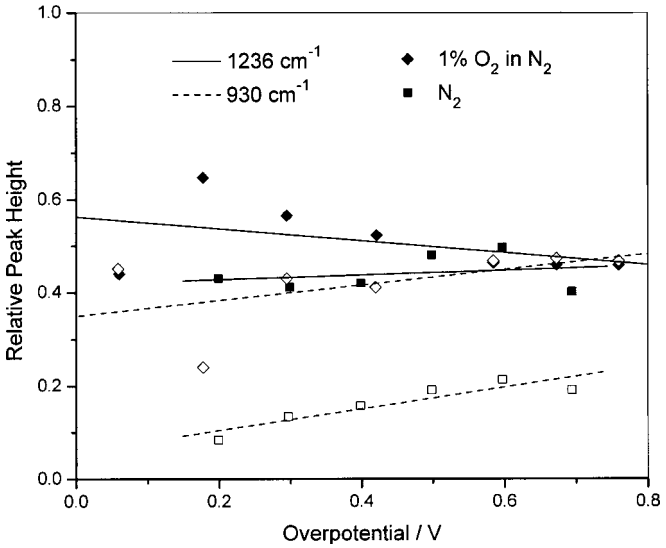

Figure 6. Peak heights as a function of overpotential relative to 1124 cm^{-1} band. Diamond and square symbols denote 1% O_2 in N_2 and N_2 environments. 1236 and 930 cm^{-1} relative peak heights are denoted by solid and dashed lines, respectively.

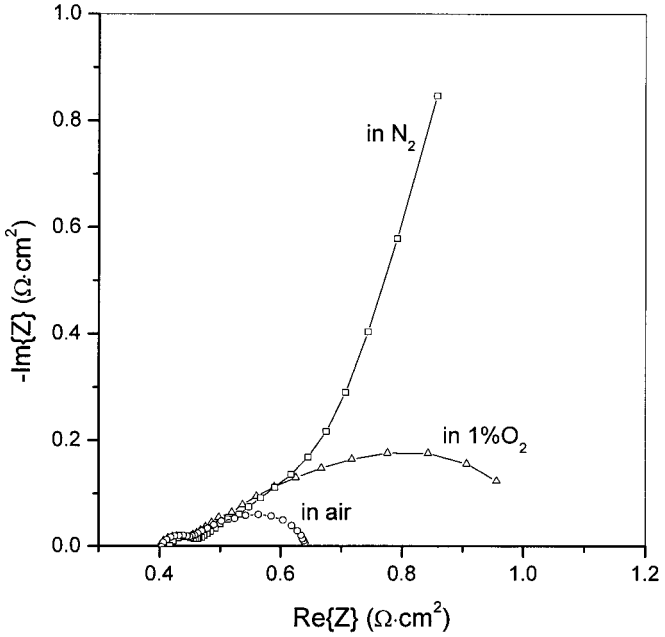

Figure 7. Impedance spectra of a symmetrical cell, SSC|SDC|SSC, measured at 550°C in air, 1% O_2, and N_2.

the disappearance of these surface oxygen species. This effect became stronger in atmospheres containing less oxygen. If the peak heights for the strongest mode, O_2^- (1124 cm^{-1}), are compared across the three feed gases for an overpotential of ~300 mV, a trend can be seen. For the oxygen rich case (air), this mode has a peak height of 0.15; for 1% O_2 in N_2, the peak height at an equivalent overpotential is 0.6; and for the trace oxygen case (N_2), the peak height is 0.9. This trend 1:4:6 in peak heights for air: 1% O_2 in N_2:N_2 can be contrasted with the kinetic data, where the reduction currents are 920:160:1.

The features under conditions of higher oxygen concentration at the electrode surface are smaller than those when the oxygen concentration is severely limited. This is because there is not enough oxygen in the gas phase to replace the surface oxygen species, which are removed by applying cathodic overpotentials, under the oxygen-deficient conditions. The interfacial polarization increases, as the rate-determining step becomes the supply of reactive adsorbate at the oxide surface. The trends shown in Fig. 6 would also seem to indicate that two different adsorbates are involved in the overall reduction pathway.

Shown in Fig. 7 are the impedance spectra of a symmetrical SSC/SDC/SSC cell measured in air, 1% O_2 in N_2, and N_2. The bulk resistance of the electrolyte remained constant at about 0.4 Ω cm^2 while the interfacial polarization resistance between the SSC electrode and SDC electrolyte increased significantly as the gas was switched from air to 1% O_2 and to N_2. The contribution of mass transfer or charge transfer to interfacial polarization can be quantitatively studied using the combination of *in situ* pd-FTIRES and impedance spectroscopy. Shown in Fig. 8 are the typical impedance spectra of an SSC/SDC/SSC interface measured in 1% O_2 at 550°C under the influence of the dc polarization, whereas the corresponding pd-FTIRES spectra under the identical conditions for these impedance measurements were shown in Fig. 3b. Each impedance spectrum consists of two arcs, in which the low frequency arc shrunk rapidly with increasing the dc polarization, implying that this arc is closely related to the charge-transfer process, not the mass-transfer process. The size of the high frequency arc was relatively insensitive to the applied dc polarization, suggesting that this arc corresponds primarily to the bulk transport. Since the sizes of the low frequency arcs were much greater than those of the high frequency arcs, the rates of the overall interfacial processes are controlled mainly by the charge-transfer processes under these conditions. This is consistent with the pd-FTIRES results as discussed earlier. Further details will be discussed in a subsequent communication.[15]

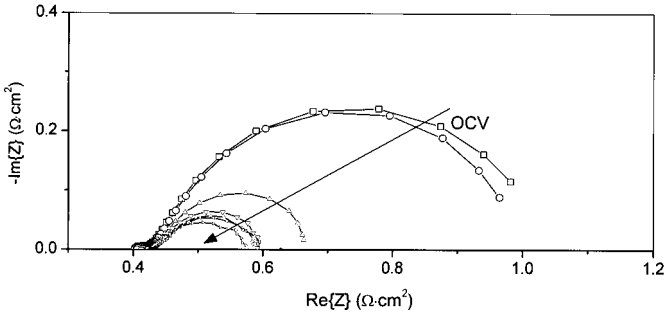

Figure 8. Effect of dc polarization on the impedance responses measured at 550°C in 1% O_2. The arrow indicates the increasing direction of the dc bias from 0 to 1.1 V with 0.2 V increment. The corresponding pd-FTIRES spectra under the identical conditions for these impedance measurements are shown in Fig. 3b.

Conclusions

In situ potential dependent FTIR emission spectroscopy is capable of probing gas/solid interactions as electrochemical reactions take place under practical conditions for fuel cell operation, providing valuable information on surface chemistry and electrochemical processes of the cathodes without any modification. Using *in situ* pd-FTIRES we have found evidence for two, possibly three distinct dioxygen species present on the electrode surface. Broad spectral features are assigned to the electrochemical polarization-induced changes in the optical properties of the electrode surface layer. This, to the authors' best knowledge, is the first report of infrared electroemission.

The combination of *in situ* potential-dependent FTIR emission spectroscopy (pd-FTIRES) and impedance spectroscopy (IS) will be a very powerful tool for investigating mechanisms of oxygen reduction, allowing direct correlation between the phenomenological behavior of an electrode (as determined by IS) and its surface molecular structures (as revealed by pd-FTIRES) under the actual fuel cell operating conditions. This will provide us with information that has never before been accessible, which is invaluable to rational design of better catalysts/cathodes for oxygen reduction. Further, the theory and methodology developed for study of cathodes are also being applied to the study of anodes in order to achieve rational design of contaminant-tolerant anodes for SOFCs (to avoid carbon deposition and sulfur poisoning).

Acknowledgments

The authors would like to thank Dr. Richard Jackson at Bruker Optics, Inc., for useful discussions and suggestions, and Milan Milosevic at Harrick Scientific, Inc., for discussions on optical accessories. The authors also gratefully acknowledge the technical discussions with Dr. Lane Wilson at DOE and the financial support of this research by National Science Foundation (grant CTS-9819850), DoE-NETL (grant DE-FG26-01NT41274), the DARPA/DSO Palm Power program directed by Dr. Robert Nowak and funded through ARMY/ARO grant DAAD19-01-1-0649 monitored by Dr. Richard Paur, and the Georgia Institute of Technology Molecular Design Institute under prime contract N00014-95-1-1116 from the Office of Naval Research.

Georgia Institute of Technology assisted in meeting the publication costs of this article.

References

1. C. Xia and M. Liu, *Adv. Mater.*, **14**, 521 (2002).
2. C. Xia, F. Chen, and M. Liu, *Electrochem. Solid-State Lett.*, **4**, A52 (2001).
3. J. Ryczkowski, *Catal. Today*, **68**, 263 (2001).
4. W. Suëtaka, *Surface Infrared and Raman Spectroscopy: Methods and Applications*, Chap. 4, p. 163, Plenum Press, New York (1995).
5. D. H. Sullivan, W. C. Conner, and M. P. Harold, *Appl. Spectrosc.*, **46**, 811 (1992).
6. C. Korzeniewski, in *Critical Reviews in Analytical Chemistry*, Vol. 27, p. 81, CRC Press, Inc., Boca Raton, FL (1997).
7. C. Xia and M. Liu, *J. Am. Ceram. Soc.*, **84**, 1903 (2001).
8. M. Handke and N. J. Harrick, *Appl. Spectrosc.*, **40**, 401 (1986).
9. J. D. E. McIntyre, in *Advances in Electrochemistry and Electrochemical Engineering*, P. Delahy and C. W. Tobias, Editors, Vol. 9, p. 61, Wiley, New York (1973).
10. M. Che and A. J. Tench, in *Advances in Catalysis*, Vol. 32, p. 1, Academic Press, New York, (1983).
11. A. Bielański and J. Haber, *Oxygen in Catalysis*, Marcel Dekker, Inc., New York (1991).
12. A. A. Davydov, *Infrared Spectroscopy of Adsorbed Species on the Surfaces of Transition Metal Oxides*, Wiley, Chichester, U.K. (1990).
13. M. Che, K. Dyrek, M. Kermarec, and A. J. Tench, *Rev. Chim. Miner.*, **21**, 669 (1984).
14. P. J. Gellings and H. J. M. Bouwmeester, *Catal. Today*, **12**, 1 (1992).
15. X. Lu, P. Faguy, and M. Liu, Unpublished work.